Reshak and Azam, J Material Sci Eng 2014, 3:2
DOI: 10.4172/2169-0022.1000139

Journal of Material Sciences & Engineering

Research Article **Open Access**

Electronic Structure and Thermal Study of Ag_3PS_4 and $Ag_5PS_4Cl_2$ from Direct to Indirect Energy Gap

Reshak AH[1,2] and Sikander Azam[1]*

[1] *New Technologies- Research Center, University of West Bohemia, Univerzitni 8, 306 14 Pilsen, Czech Republic*
[2] *Center of Excellence Geopolymer and Green Technology, School of Material Engineering, University Malaysia Perlis, 01007 Kangar, Perlis, Malaysia*

Abstract

The band structure and density of states of the orthorhombic Ag_3PS_4 and $Ag_5PS_4Cl_2$ compounds has been investigated. The calculations are derived from the total-energy calculations using the Full Potential-Linearized Augmented Plane Wave (FPLAPW) method. The exchange and correlation potential is treated by the Local Density Approximation (LDA), Generalized Gradient Approximation (GGA) and Engel Vosko GGA. From the study of the band structure we confirmed that the Valence Band Maximum (VBM) and Conduction Band Minimum (CBM) of Ag_3PS_4 compounds situated at Γ point, indicating a direct band gap. While for $Ag_5PS_4Cl_2$ compound the VBM occurs along the Z–S direction and CBM at Γ point exhibiting indirect band gap. The partial density of states confirm that the lower part of the valence band is dominated by S-s orbital, the mid part by P-s orbital and the VBM by the Ag-d orbital. The conduction band consists the major contribution of Ag-s/p orbital. Furthermore, the thermoelectric properties of both compounds were investigated by means of BoltzTraP code. The electrical conductivity, electrical resistivity, the power factor and Seebeck coefficient were investigated in the temperature range from 300 to 800 K. The electrical conductivity was enhanced by increasing the temperature, which leads to a small electrical resistivity and a large Seebeck coefficient. Consequently, large values of about 3.75×10^{11} and 1.2×10^{11} W/m K^2 for Ag_3PS_4 and $Ag_5PS_4Cl_2$ compounds were obtained. Therefore, the thermoelectric property of Ag_3PS_4 is not as good as that of $Ag_5PS_4Cl_2$. Therefore, it can be concluded that $Ag_5PS_4Cl_2$ is suitable for high performance thermoelectric application than Ag_3PS_4 at higher temperature.

Keywords: Band structure; Density of states; Thermoelectric properties; DFT

Introduction

The most critical issues which arises the energy consumption along with the environmental pollution. In traditional fossil fuel machinery, as much as 70% of the energy is wasted heat related entropy [1]. Due to this glaring, the thermoelectric material has been spread out to be a broadly researched field, with the reason that they can animate the waste heat to electricity directly. These properties (thermoelectric properties) are explicit by the figure of merit (ZT) as , $ZT=\frac{S^2\sigma}{\kappa}T$ (S is the Seebeck coefficient, σ - electrical conductivity, κ - thermal conductivity, and T is the absolute temperature). To obtain the high energy conversion efficiency requires a larger value of ZT. In spite of this, enhancing the highly coupled limitations of $ZT=\frac{S^2\sigma}{\kappa}T$, concurrently possess a tough challenge. In 1995 the "Phonon Glass, Electron Crystal" (PGEC) concept has been set up, which refers to a model thermoelectric material, possessing the thermal properties analogous to an amorphous solid even as its electrical properties are related to a single crystal semiconductor [2]. The most investigated class (PGEC) is clathrates [3,4]. The transition metal thiophosphates produces a variety of appealing class of compounds, which are focal point for the researchers for the reason of its numerous structural chemistries along with their physical properties [5].

The $AuPS_4$ compound [6] is the only ternary thiophosphate of gold, a number of compounds relating to the ternary Ag-P-S and Cu-P-S system have stated in the text, e.g. $Ag_4P_2S_6$ [7], $Ag_4P_2S_7$ [8], $Ag_7P_3S_{11}$ [9,10], Cu_3PS_4 [11] and $CuPS_2$ [12]. Besides this there is general formula for argyrodite family $(A^{m+})_{(12-n-m/m}B^{n+}(X^{2-})_{6-y}(Z^-)_y$ ($A=Ag^+$, Cu^+, etc.; $B=P^{5+}$, Ge^{4+}, etc.; X= S, Se, Te; Z=Cl, Br, I), which has got its identity from the mineral compound Ag_8GeS_6. The formula of Ag^+ ions, pentavalent phosphorus, and S^{2-} ions is limited to $Ag_{7-y}PS_{6-y}Z_y$. Typical for the crystal structures is an anion framework of interpenetrating, centered icosahedra providing ideal and distorted tetrahedral cation sites [13]. In comparison to the other materials, these materials are of significance due to their high ionic conductivity, which take places at high temperature polymorphic appearances of silver or copper enclosing compounds [14-17]. In addition quite a lot of compounds, e.g. $Ag_6GeS_4Br_2$ [18] exist matching with the formula of argyrodites but producing other types of structures. As a result of high ionic conductivity of several silver enclosing thiophosphates, Stefan et al. [19] have initiated with the syntheses of associated compounds. They worked on the two innovative thiophosphatechlorides $Ag_5PS_4Cl_2$ and $Ag_{15}(PS_4)_4Cl_3$. Besides, the Ag_3PS_4 compound crystal structure, derived by X-ray powder methods [20] was also assured by single-crystal.

From above, no comprehensive work neither experimental data nor first principles calculations on the structural, electronic, optical and thermoelectric properties of Ag_3PS_4 and $Ag_5PS_4Cl_2$ compounds have appeared in the literature. Therefore as a natural extension to previous experimental work a detailed depiction of the structural, electronic, optical and thermoelectric properties of Ag_3PS_4 and $Ag_5PS_4Cl_2$ compounds using full potential method is timely and would

---

***Corresponding author:** Sikander Azam, New Technologies- Research Center, University of West Bohemia, Univerzitni 8, 306 14 Pilsen, Czech Republic, Tel: +420-377-631-111; E-mail: sikander.physicst@gmail.com

Received July 14, 2014; **Accepted** September 17, 2014; **Published** September 24, 2014

Citation: Reshak AH, Azam S (2014) Electronic Structure and Thermal Study of Ag_3PS_4 and $Ag_5PS_4Cl_2$ from Direct to Indirect Energy Gap. J Material Sci Eng 3: 139. doi:10.4172/2169-0022.1000139

bring us important insights in understanding the origin of the band structure and densities of states. Hence it is very important to use a full potential method.

Computational Methodology

The crystal structure of Ag_3PS_4 and $Ag_5PS_4Cl_2$ compounds has been shown in Figure 1. The compound has the orthorhombic structure with space group #31 ($P\,m\,n\,2_1$) and #38 ($A\,m\,m\,2$). The lattice constants for Ag_3PS_4/$Ag_5PS_4Cl_2$ compounds are a = 7.647(3)/7.409(1) Å, b = 6.858(2)/ 11.143(2) Å, c = 6.506(1)/ 6.258(1) Å, [19]. The electronic structure of both Ag_3PS_4 and $Ag_5PS_4Cl_2$ compounds are deliberated by means of the full potential linearized augmented plane wave as executed in the WIEN2k code [21]. We have performed the DFT calculations utilizing the self-consistent full-potential LAPW method [22]. The exchange correlation potential E_{xc} was appraised by means of local density approximation (LDA), generalized gradient approximation (GGA) and EVGGA as amended by Engel Vosko [23-25]. The ι-expansions of the wave functions were deprived out up to ι_{max}=10 within the muffin-tin spheres of radius R_{MT}. While the Fourier expansion for the charge density was expanded up to $G_{max=}$12. In the interstitial regions the wave functions were expanded in the plane waves for the cut off of $K_{MAX} \times R_{MT}$ = 7.0, in sequence to accomplish the convergence for energy eigenvalues. The valves for muffin-tin radii R_{MT} was chosen for Ag_3PS_4 compound, R_{MT} (Ag) =2.37 a.u. and R_{MT} (S and P) =1.82 a.u. and for $Ag_5PS_4Cl_2$ compound, R_{MT} (Ag) =2.39 a.u., R_{MT} (S and P) =1.84 a.u. and R_{MT} (Cl) =2.16 a.u. In additional, we also have calculated the Seebeck coefficient, electrical conductivity, the power factor and the resistivity by using BoltzTraP code [26].

Results and Discussion

Electronic structure

The calculated electronic band structures along the high symmetry directions Y-Z-G-X-S-Y and Z-S-G-Y-G-Z for Ag_3PS_4 and $Ag_5PS_4Cl_2$ compounds are plotted in Figure 2. It is clear from Figure 2 that the bands in the $Ag_5PS_4Cl_2$ compound are dispersive compared to Ag_3PS_4 compound. The band dispersion in the $Ag_5PS_4Cl_2$ compound indicates that the effective mass of the holes and electron will be larger than Ag_3PS_4 but the electron and hole mobility will be smaller than Ag_3PS_4. One of the parameters of interest in semiconductors that can be determined from the band structure is the fundamental band gap Eg, which is the difference of energies of the bottom most Conduction Band (CB) and topmost Valance Band (VB). It can be seen that the Valence Band Maximum (VBM) and Conduction Band Minimum (CBM) of Ag_3PS_4 compounds occurs along the Γ point, showing the direct band gap. While for $Ag_5PS_4Cl_2$ compound the VBM occurs along the Z–S direction and the CBM occurs Γ points resulting the indirect band gap. The calculated band gap of Ag_3PS_4 ($Ag_5PS_4Cl_2$) are equal to 1.57 (1.69) eV for LDA, 1.73 (1.81) eV for GGA and 1.81 (1.95) eV for EVGGA.

These values are expected to be smaller than the experimental values as expected from DFT. To the best of our knowledge, there are no previous experimental or theoretical data for the energy band gaps available in literature to make a meaningful comparison. The calculated Total Densities of States (TDOS) for Ag_3PS_4 and $Ag_5PS_4Cl_2$ are presented in Figure 3. The VB for Ag_3PS_4 and $Ag_5PS_4Cl_2$ consists of four major regions. As demonstrated below, by the analysis of orbital and site Projected DOS (PDOS), the lowest energy region of the VB in the energy range -13.5 to -12.5 eV (to be called VB1 hereafter) of Ag_3PS_4 and $Ag_5PS_4Cl_2$ comes from the S-s and P-p states. The energy region located above VB1 to be called as the VB2 is in the energy range from -9.5 to -8.5 eV. It is split into narrow sharp sub-bands. The other region is VB3 located at higher energies than VB2 and it covers the range from -6.5 to 5.5 eV, it is localized and narrow. The topmost part of the VB is the fourth region to be denoted as VB4. It is located in a broad energy range ~ -4.5 to 0.0 eV.

It is seen that VB2 of both compounds consists of P-s and S-p states with small contribution of the Ag-s/p and S-s states. In VB2 region there exits a strong hybridization between s and p states of P and S atoms. The last region (VB3) consists of very sharp peaks centered at -6.5 to -5.5 eV, which are coming from P-p and S-p states. The topmost part of the VB, called VB4, consists of two parts: the first one is located at lower energies. Strong contribution to VB4 is coming from P-p, S-p and Cl-s/p orbitals along with the small contribution of Ag-s orbital. The CB edge is well dispersed and consists of the major contribution of Ag-s/p orbitals.

Thermoelectric Properties

The thermopower (S), electronic conductivity (σ), power factor (PF) and resistivity (ρ) were obtained by using the semi-classical Boltzmann theory in conjunction with rigid band and constant relaxation time approximations [26]. All the calculations of transport properties were implemented in the BoltzTraP package [26].

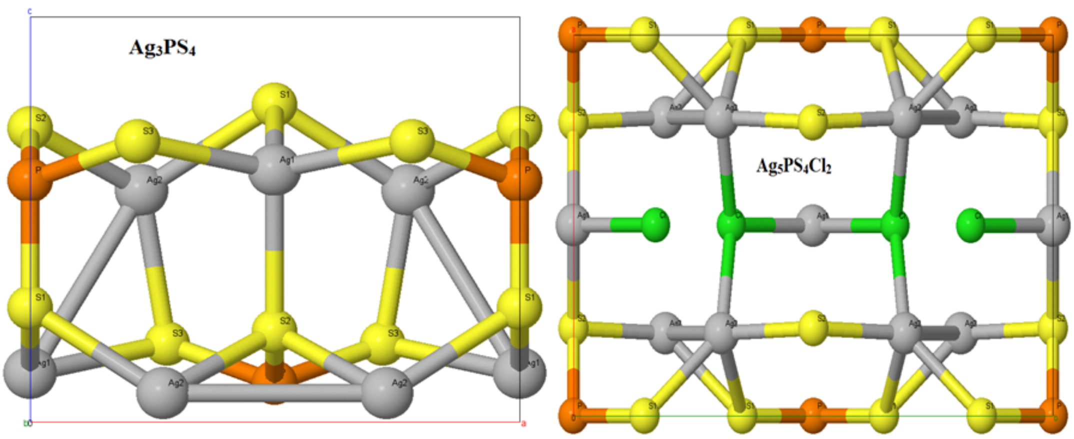

Figure 1: Unit cell structure.

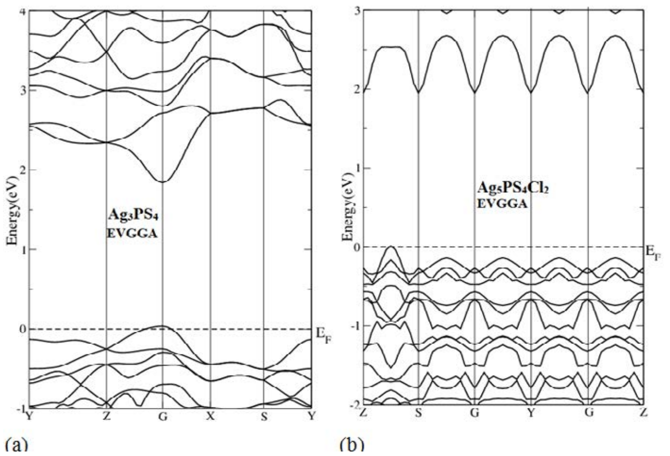

Figure 2: Calculated band structure.

To calculate the electrical conductivity values (σ) of the two compounds, we must determine the relaxation time τ. Here, we adopt the strategy previously used by Ong et al. [27] for calculating the thermoelectric properties of ZnO. They assume that the relaxation time τ is direction independent, and treat relaxation time as a constant.

Figure 4a presents the temperature dependence of electrical conductivity from 300 K to 800 K for Ag_3PS_4 and $Ag_5PS_4Cl_2$. It was observed the electrical conductivity increases with increasing the temperature from 300 to 800K, indicating a typical semiconductor behavior. As the temperature increases from room temperature, the electrical conductivities increases gradually, displaying the characteristic of degenerate semiconductors, owing to reduced mobility [28]. Some electrons in the deep energy level may be thermally activated at elevated temperature to participate in the transport. The electrical conductivity of Ag_3PS_4 was lower than that of $Ag_5PS_4Cl_2$. It is well known that the conductivity depends on the carrier mobility μ and carrier concentration n, i.e. σ = μne.

The large band dispersion indicates the high electrical conductivity for the $Ag_5PS_4Cl_2$ than Ag_3PS_4, which leads to approximate one-dimensional electron transport. And also the higher electrical conductivity of $Ag_5PS_4Cl_2$ may be a result of full densification of material.

Such transition at higher temperature in terms of the electrical conductivity and Seebeck coefficient was also observed by Iida et al. [29,30]. The temperature dependences of the Seebeck coefficient is illustrated by Figure 4b. The S values of Ag_3PS_4 and $Ag_5PS_4Cl_2$ compounds are positive, confirming the p-type nature of the compounds. As the temperature increases, the value of the Seebeck coefficient graph for the two compounds also increases. Among the two compounds the Ag_3PS_4 has the smallest Seebeck coefficient, whereas $Ag_5PS_4Cl_2$ has the largest within the entire temperature range. The number of hole bands near the Γ point of BZ for Ag_3PS_4 and near Z-S-G-Y-G-Z points of BZ in $Ag_5PS_4Cl_2$ is large. Thus, the hole density is very large. For the high density of local holes existing, holes are the main carrier dominates the electrical transport. So, the calculated p-type Seebeck coefficient should be more significant in practice.

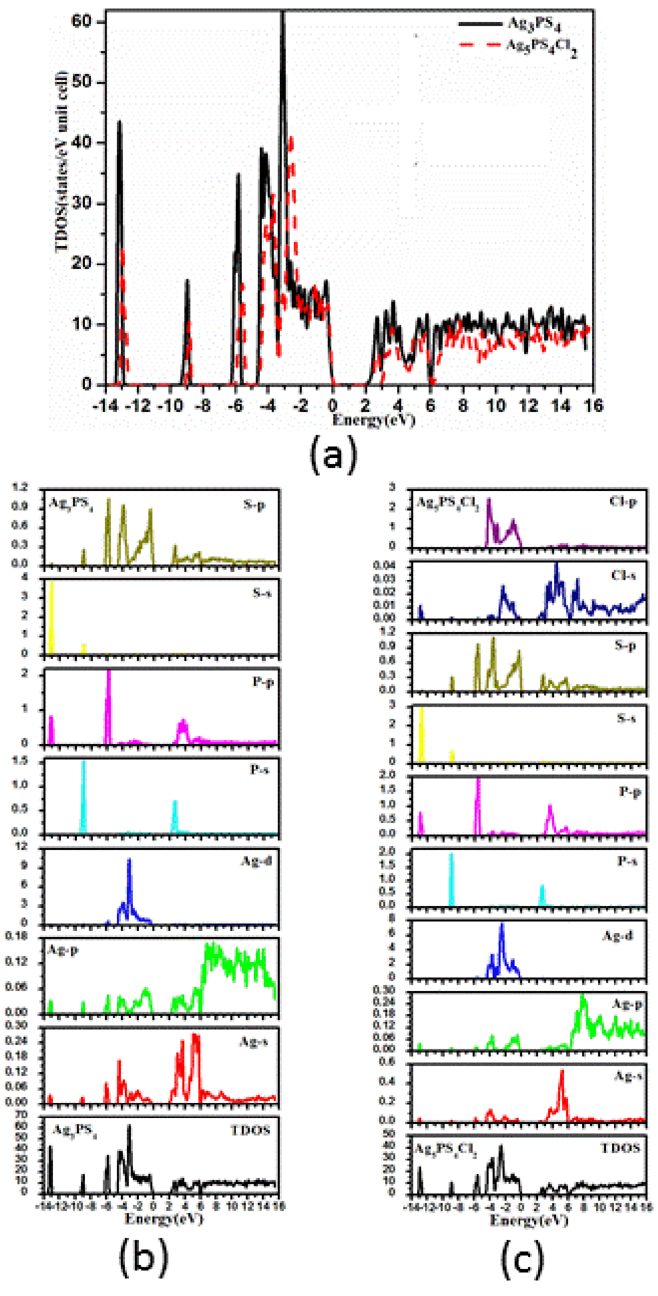

Figure 3: Calculated total and partial densities of states (States/eV unit cell).

The anisotropy of the electronic band structure of the two compounds means the strong anisotropy of electronic transport properties: the strong van der Waals force, the highly localized hole band, and the strong dispersion of electronic bands. Anisotropic electronic structure ensures low dimensional of carrier transport, and the localized hole band is detrimental to the effect of electron–hole compensation for Seebeck coefficient.

The power factor of the two investigated compounds has been shown in Figure 4c. $Ag_5PS_4Cl_2$ has a higher level of power factor in comparison with Ag_3PS_4 within the entire temperature range. To maximize the power factor, the electrical conductivity and the Seebeck coefficient need to be high. In this case the power factor for $Ag_5PS_4Cl_2$ is higher than that for Ag_3PS_4. The power factor is one of the important thermoelectric parameters which determines the thermoelectric energy conversion, is defined as $S^2\sigma$. The room-temperature power factors increase from 4.5×10^{10} and 1.0×10^{11} W/m K2 for Ag_3PS_4 and $Ag_5PS_4Cl_2$

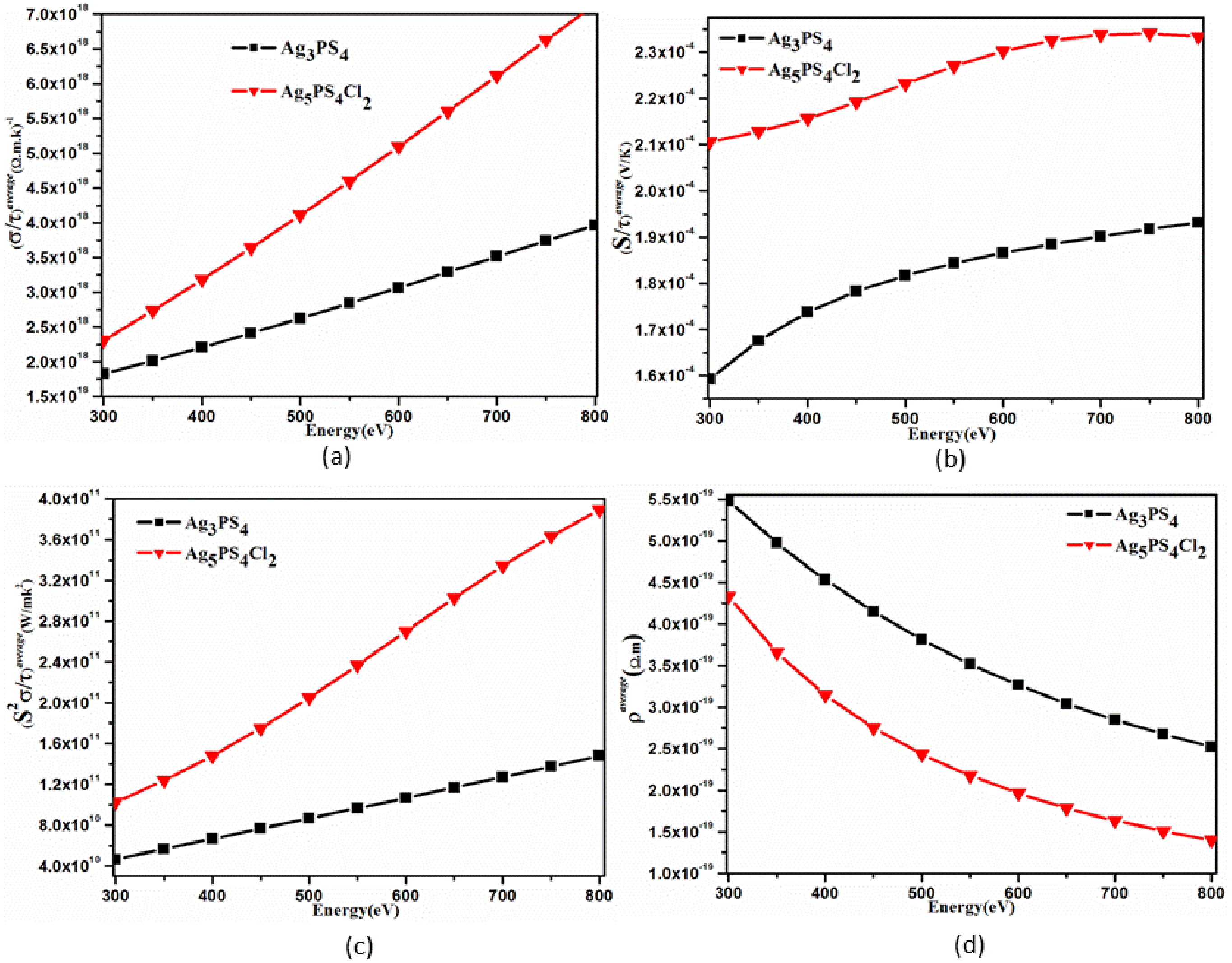

(a) (b) (c) (d)

Figure 4: Calculated average thermoelectric properties; Seebeck coefficients, electrical conductivity and thermal conductivity.

compounds. It indicates that the power factor of $Ag_5PS_4Cl_2$ is higher than that of Ag_3PS_4. The PF of both compounds is increasing with the increase in temperature. Also Ag_3PS_4 compound has less Seebeck coefficient value than of $Ag_5PS_4Cl_2$ compound through the whole range of temperature. Therefore, the thermoelectric property of Ag_3PS_4 compound is not as good as that of $Ag_5PS_4Cl_2$ compound. Therefore, it can be concluded that $Ag_5PS_4Cl_2$ is suitable for high performance thermoelectric application than Ag_3PS_4 at higher temperature. The power factor of both compounds is enhanced greatly when the temperature increases above 300 K. Since the power factor is a comprehensive outcome of the Seebeck coefficient and conductivity, the PF value of both compound is much different at moderate temperature range. They have an optimal power factor of 3.75×10^{11} and 1.2×10^{11} W/m K^2 for Ag_3PS_4 and $Ag_5PS_4Cl_2$ compounds due to a high Seebeck coefficient of 2.35×10^{-4} and 1.9×10^{-4} VK^{-1}, a moderate resistivity of 1.4×10^{-19} and 2.5×10^{-19} Ωm at 800 K, respectively.

Considering the stability of the specimens, we have measured TE properties in the 300–800 K temperature range. The temperature dependence of resistivity for both compounds is shown in Figure 4d. The ρ value of both compounds decreases with increasing temperature ($d\rho/dt<0$) indicate that both compounds possesses thermal active semiconducting behavior [31].

We thus speculate the reason of the transition (holes concentration p) is that, that conductivity spectra $Ag_5PS_4Cl_2$ compound is greater than the Ag_3PS_4. This is to say, that the holes doping in this system, which can explain the obvious decrease of both electrical resistivity ρ as shown in Figure 4d.

Conclusion

We have used the FP-LAPW method to calculate the band structure and density of states of Ag_3PS_4 and $Ag_5PS_4Cl_2$ compounds. The calculation confirms that Ag_3PS_4 has the direct band gap while the $Ag_5PS_4Cl_2$ possess indirect band gap. The partial density of states show that the lower part of the valence band is formed by S-s orbital, the mid part by P-s orbital while the VBM is originated from Ag-d orbitals. While the conduction band consists of the major contribution of Ag-s/p orbitals. The transport parameters provide evidence of an increase in hole concentration. Electrical conductivity and Seebeck coefficient were calculated at high temperatures to elucidate the thermoelectric properties. Both of Ag_3PS_4 and $Ag_5PS_4Cl_2$ compounds exhibit p-type semi conducting. We found the robust dependence of temperature on power factor. Its maximum, however, located at higher temperatures. The electrical conductivity was enhanced by increasing the temperature, which leads to a small electrical resistivity and a large Seebeck coefficient. Consequently, large values of about 3.75×10^{11} and 1.2×10^{11} W/m K^2 for Ag_3PS_4 and $Ag_5PS_4Cl_2$ compounds were obtained. Therefore, the thermoelectric property of Ag_3PS_4 is not as good as that of $Ag_5PS_4Cl_2$. Therefore, it can be concluded that $Ag_5PS_4Cl_2$ is suitable for high performance thermoelectric application than Ag_3PS_4 at higher temperature.

Acknowledgement

The result was developed within the CENTEM project, reg. no. CZ.1.05/2.1.00/03.0088, co-funded by the ERDF as part of the Ministry of Education, Youth and Sports OP RDI programme.

References

1. Biswas K1, He J, Blum ID, Wu CI, Hogan TP, et al. (2012) High-performance bulk thermoelectrics with all-scale hierarchical architectures. Nature 489: 414-418.
2. Slack GA (1995) New Materials and Performance Limits for Thermoelectric Cooling, CRC Press, Boca Raton, USA.
3. Nolas GS, Cohn JL, Slack GA, Schujman SB (1998) Semiconducting Ge clathrates: Promising candidates for thermoelectric applications. Appl Phys Lett 73: 178.
4. Nolas GS, Slack GA, Schujman SB (2001) Chapter 6 Semiconductor clathrates: A phonon glass electron crystal material with potential for thermoelectric applications. Semiconduct Semimet 69: 255-300.
5. Villars P, Calvert LD (1997) Pearson's Handbook of Crystallographic Data for Intermetallic phases. (2ndedn). ASM, Metals Park.
6. Jorgens S, Johrendt D, Mewis A, Anorg A (2003) Allg Chem 629: 2236.
7. Toffoli P, Khodadad P, Rodier N (1983) Structure dune deuxieme variete dhexathiodiphosphate(IV) dargent, $Ag_4P_2S_6$. Comparaison des structures des deux varieties. Acta Crystallogr C39: 1485-1488.
8. Toffoli P, Khodadad P, Rodier N (1977) Structure cristalline du pyrothiophosphate dargent, $Ag_4P_2S_7$. Acta Crystallogr B33: 1492-1494.
9. Toffoli P, Khodadad P, Rodier N (1982) Structure du tetrathiomonophosphate(V) heptathiodiphosphate(V) dargent. Acta Crystallogr B38: 2374.
10. Brinkmann C, Eckert H, Wilmer D, Vogel M, der Gunne JSA (2004) Re-entrant phase transition of the crystalline ion conductor $Ag_7P_3S_{11}$. Solid State Sci 6: 1077.
11. PfitznerA, Reiser S, Kristallogr Z (2002) 217: 51.
12. Kom JK, Flahaut J, Domange L, Seances CD (1963) Acad. Sci. Paris 257: 3919.
13. Kuhs WF, Nitsche R, Scheunemann K (1979) Mater Res Bull 14: 241-248.
14. Wada H (1992) Crystal structures and silver ionic conductivities of the new compounds Ag_7NbS_6, Ag_7TaSe_6 and $Ag_{7-\xi}TaSe_{6-\xi}I_\xi$ $(0.1 \leqslant \xi \leqslant 0.5)$ J Alloys Compd 178: 315.
15. Gaudin E, Boucher F, Petricek V, Taullele F, Evain M (2000) Structures and phase transitions of the A_7PSe_6 (A=Ag, Cu) argyrodite-type ionic conductors. III. α-Cu_7PSe_6. Acta Crystallogr B56: 972-979.
16. Gagor A, Pietraszko A, Kaynts D (2005) Diffusion paths formation for Cu^+ ions in superionic Cu_6PS_5I single crystals studied in terms of structural phase transition. J Solid State Chem 178: 3366-3375.
17. T. Nilges, A. Pfitzner, Z. Kristallogr. 220 (2005) 281.
18. Wagener M, Deiseroth HJ, Engelen B, Reiner C, Kristallogr Z Suppl. 20 (2003) 156.
19. Jorgens S, Mewis A (2007) $Ag_5PS_4Cl_2$ and $Ag_{15}(PS_4)_4Cl_3$-Crystal structures and their relation to Ag_3PS_4. Solid State Sciences 9: 213-217.
20. Andrae H, Blachnik R (1992) Metal sulphide-tetraphosphorusdekasulphide phase diagrams. J Alloys Compd 189: 209-215.
21. Blaha P, Schwarz K, Luitz J (1999) WIEN97, A full potential linearized augmented plane wave package for calculating crystal properties, Karlheinz Schwarz. Techn. Universit at Wien, Austria.
22. Jansen HJF, Freeman AJ (1984) Total-energy full-potential linearized augmented-plane-wave method for bulk solids: Electronic and structural properties of tungsten. Phys Rev B 30: 561.
23. Perdew JP, Zunger A (5048) Self-interaction correction to density-functional approximations for many-electron systems. Phys Rev B 23: 5048.
24. Perdew JP, Burke K, Ernzerhof M (1996) Generalized Gradient Approximation Made Simple Phys Rev Lett 77: 3865.
25. Engel E, Vosko SH (1994) Fourth-order gradient corrections to the exchange-only energy functional: Importance of. Phys Rev B Condens Matter 50: 10498-10505.
26. Madsen GKH, Singh DJ (2006) BoltzTraP. A code for calculating band-structure dependent quantities. Comput Phys Commun 175: 67.
27. Ong KP, Singh DJ, Wu P (2011) Analysis of the thermoelectric properties of n-type ZnO. Phys. Rev. B 83: 115110.
28. Bux SK, Yeung MT, Toberer ES, Snyder GJ, Kaner RB, et al. (2011) Mechanochemical synthesis and thermoelectric properties of high quality magnesium silicide. J Mater Chem 21: 12259-12266.
29. Sakamoto T, Iida T, Fukushima N, Honda Y, Tada M, et al. (2011) Thermoelectric properties and power generation characteristics of sintered undoped n-type Mg2Si. Thin Solid Films 519: 8528-8531.
30. Nemoto T, Iida T, SATO J, Oguni Y, Matsumoto A, et al. (2010) Characteristics of a Pin–Fin Structure Thermoelectric Uni-Leg Device Using a Commercial n-Type Mg2Si Source. J Electron Mater 39: 1572-1578.
31. Kosuga A, Plirdpring T, Higashine R, Matsuzawa M, Kurosaki K, et al. (2012) Appl Phys Lett.